

LAWRENCE
LIVERMORE
NATIONAL
LABORATORY

UCRL-CONF-231548

Simulation of Enhanced-Explosive Devices in Chambers and Tunnels

J. B. Bell, A. L. Kuhl, V. E. Beckner

June 6, 2007

High Performance Computing Conference
Pittsburg, PA, United States
June 18, 2007 through June 22, 2007

Disclaimer

This document was prepared as an account of work sponsored by an agency of the United States Government. Neither the United States Government nor the University of California nor any of their employees, makes any warranty, express or implied, or assumes any legal liability or responsibility for the accuracy, completeness, or usefulness of any information, apparatus, product, or process disclosed, or represents that its use would not infringe privately owned rights. Reference herein to any specific commercial product, process, or service by trade name, trademark, manufacturer, or otherwise, does not necessarily constitute or imply its endorsement, recommendation, or favoring by the United States Government or the University of California. The views and opinions of authors expressed herein do not necessarily state or reflect those of the United States Government or the University of California, and shall not be used for advertising or product endorsement purposes.

This work was performed under the auspices of the U. S. Department of Energy by University of California, Lawrence Livermore National Laboratory under Contract W-7405-48

Simulation of Enhanced-Explosive Devices in Chambers and Tunnels

John B. Bell*
Lawrence Berkeley National Laboratory
Berkeley, CA USA

Allen L. Kuhl
University of California Lawrence Livermore National Laboratory
Livermore, CA USA

Vincent E. Beckner
Lawrence Berkeley National Laboratory
Berkeley, CA USA

Summary

Introduction: Shock-dispersed fuel (SDF) explosives use a small chemical charge to disperse a combustible fuel that burns in the post-detonation environment. The energy released in the combustion process has the potential for generating higher pressures and temperatures than conventional explosives. However, the development of these types of novel explosive systems requires a detailed understanding of all of the modes of energy release.

Objective: The objective of this project is develop a simulation capability for predicting explosion and combustion phase of SDF charges and apply that capability to quantifying the behavior of these types of explosives.

Methodology: We approximate the dynamics of an SDF charge using high Reynolds number, fast chemistry model that effectively captures the thermodynamic behavior of SDF charges and accurately models the key modes of energy release. The overall computational model is combined with Adaptive Mesh Refinement (AMR) , implemented in a parallel adaptive framework suited to the massively parallel computer systems.

Results: We have developed a multiphase version of the model and used it to simulate an SDF charge in which the dispersed fuel is aluminum flakes. Flow visualizations show that the combustion field is turbulent for the chamber and tunnel cases studied. During the 3 milli-seconds of simulation, over 90% of the Al fuel was consumed for the chamber case, while about 40% was consumed in the tunnel case in agreement with Al-SDF experiments.

Significance to DoD: DoD has a requirement to develop enhanced energetic materials to support future military systems. The SDF charges described here utilize the combustion mechanism to increase energy per gram of fuel by a factor of 7 to 10 over conventional (detonating) charges, and increase the temperature of the explosion cloud to 2,000 - 4,000 K (depending on the SDF fuel). Accurate numerical simulation of such SDF explosions allows one to understand the energy release mechanism, and thereby design full-scale systems with greatly improved explosive efficiency.

Approved for public release; distribution is unlimited.

*Corresponding author, jbbell@lbl.gov

1. Introduction

For many explosives, only a fraction of the chemical energy is released in the detonation. Calorimetry data for TNT from Ornellas [13] shows that when the ambient gas is inert, there is substantially less total energy released than when the ambient gas includes oxygen. This data indicates that burning of the explosion byproducts plays a key role in the overall energetics of the system. The basic concept of shock-dispersed fuel (SDF) charges is to directly exploit this idea. More precisely, in an SDF charge a small charge is used to disperse a fuel and create a turbulent environment in which the fuel can mix with ambient air and burn. In our previous work [2], we considered the afterburning of detonation byproducts from a mixture of TNT and PETN.

Although a variety of alternative fuels have been considered, here we focus on flake aluminum. For this problem we consider a multiphase model in which the aluminum is treated in the dilute limit as a dispersed phase. The two phases exchange mass, momentum, and energy according to inter-phase exchange terms. In previous work, we considered an an equilibrium model in which we assumed that the aluminum flakes are velocity and thermal equilibrium [6]. Here, we consider a two-phase treatment in which the phase are not assumed to be in equilibrium and include models for the tranfer of mass, momentum and energy between the phases. For this approximation, we assume that the aluminum does not burn as a solid and use an empirical relationship that converts solid aluminum into a fuel that can burn. We assume that the kinetics occurs on a time scale that is much faster than the fluid dynamical time scale, thus the combustion process is mixing limited. However, the oxidation of solid aluminum retains a finite rate character because of the relationship used to volatilize aluminum flakes.

In the next two sections, we briefly discuss the models and the numerical method used for the simulations and present the computational results. In the final section we discuss future directions our work on the development of SDF explosives.

2. Multiphase model

Basic equations

We model the evolution of the combustion field in the high Reynolds and Peclet number limit where molecular diffusion, heat conduction and viscosity are negligible. In this setting the gas phase can be described by multi-component gas dynamics

$$\begin{aligned}
\partial_t \rho + \nabla \cdot (\rho u) &= \dot{\sigma}_s && (1)\\
\partial_t \rho u + \nabla \cdot (\rho u u) + \nabla p_g &= \dot{\sigma}_s v - \dot{f}_s && (2)\\
\partial_t \rho E_g + \nabla \cdot (\rho u E_g + + p_g u) &= -\dot{q}_s + \dot{\sigma}_s E_s - \dot{f}_s \cdot v && (3)\\
\partial_t \rho Y_k + \nabla \cdot \rho u Y_k - \rho \dot{\omega}_k &= \beta_k \dot{\sigma}_s && (4)
\end{aligned}$$

where ρ, E_g, and p_g are the mixture density, energy and pressure, u is the fluid velocity, Y_k are mass fractions. The terms on the right hand side of the equation describe the phase interactions and are discussed below. For the model presented here we consider not only the combustion of aluminum but also the afterburning of the detonation products of the explosive used to disperse the aluminum. Thus, in the gas phase we consider five species, aluminum fuel (F), air (A), aluminum/air combustion products (P), driver charge detonation productions (D), and air/detonation product combustion products C. We model the reaction processes (the $\dot{\omega}_k$'s) with two irreversible reactions

$$\begin{aligned}
F + \phi_{s,AL} A &\rightarrow (1 + \phi_{s,AL}) P && (5)\\
D + \phi_{s,DP} A &\rightarrow (1 + \phi_{s,DP}) C && (6)
\end{aligned}$$

where $\phi_{s,\gamma}, \gamma = AL, DP$ denotes stoichiometric air/fuel ratios for the two reactions.

We treat the particle phase in the dilute limit, devoid of particle-particle interactions so that the pressure and sound speed in the particle phase are zero. We model the evolution of particle mass, momentum and

energy using a continuum model as described in Nigmatulin [12]:

$$\begin{aligned} \partial_t \sigma + \nabla \cdot (\sigma v) &= -\dot{\sigma}_s & (7) \\ \partial_t \sigma v + \nabla \cdot (\sigma v v) &= -\dot{\sigma}_s v + \dot{f}_s & (8) \\ \partial_t \sigma (E_s) + \nabla \cdot (\sigma v E_s) &= +\dot{q}_s - \dot{\sigma}_s E_s + \dot{f}_s \cdot v & (9) \end{aligned}$$

where σ is the particle phase density, v is the particle phase velocity and $E_s = C_s T_s + v \cdot v/2$ is the particle phase energy.

The phase interactions are given by the particle drag, $\dot{f}_s$, the heat exchange, $\dot{q}_s$. and, the mass source for particle volatilization, $\dot{\sigma}_s$. Here,

$$\dot{f}_s = \frac{3}{4} \frac{\rho \sigma}{\rho_s d_s} C_D (u - v)|u - v|$$

where $C_D = 24/Re_s + 4.4/\sqrt{Re_s}$ and $Re_s = \rho d_s |u - v|/\mu$, ρ_s is the mass density of the particles, d_s is the particle diameter, and μ is the fluid viscosity. The heat exchange is given by

$$\dot{q}_s = \frac{6\sigma}{\rho_s d_s} \left[\frac{N_u \kappa (T - T_s)}{d_s} + \epsilon k_b (T^4 - T_s^4) \right]$$

where $N_u = 2 + 0.6 P_r \sqrt{Re_s}$, κ is the thermal conductivity of the gas ϵ is gas emissivity, k_b is Boltzmann's constant, and $P_r = c_p \mu / \kappa$ is the Prandtl number. Finally, we define

$$\dot{\sigma}_s = \begin{cases} 0 & T_s < T_{vol} \\ -3\sigma(1. + 0.276\sqrt{Re_s})/t_s & T_s > T_{vol} \end{cases}$$

where T_{vol} is a volatilization temperature and $t_s = K d_s^2$. For a more detailed discussion of these interphase exchange terms, see [9].

Thermodynamics and combustion

The actual combustion processes for both aluminum and driver detonation products are fast relative to the time scale of the other physical processes in the problem, particularly in the high temperature post-detonation environment. Furthermore, since our focus is to predict basic combustion environment, much of the chemical detail is relatively unimportant. However, simply directly enforcing chemical equilibrium can fail to accurately predict the dynamics. Data from Kuhl et al. [7] and Ree et al. [15] shows that an equilibrium assumption does not give an accurate picture of the composition of gases resulting from a TNT charge. In essence, as the gases expand the behind the detonation, the temperature drops to the point that the reactions are effectively quenched and the composition is frozen.

Here, we adopt the thermodynamic model developed by Kuhl et al. [8] to describe the behavior of the detonation products and provide a simplified model for the combustion process. This approach is based on a thermodynamics analysis in the Le Chatelier diagram of specific internal energy versus temperature for the different components in the fluid mixture. With this approach we can enforce chemical equilibrium above a given temperature and enforce a frozen chemical composition below that temperature. We note that, in defining the energy, we include the chemical potential as part of the internal energy. (Thus, there is no heat-release term in the energy equation.) Consequently, chemical reactions at constant volume represent a change in composition that does not change the internal energy. For this analysis we treat the mixture as five gaseous components air (A), aluminum fuel (F) and its associated combustion products (P) and detonation driver gas (D) and its associated combustion products (C). For the analysis here, the product gas composition is determined by burning the two fuels in air at stoichiometric conditions.

The thermodynamic properties of the components gaseous components were computed using the Cheetah code [5] by Kuhl et al. [8]. The aluminum particles are modeled as having a fixed specific heat. When constructing the thermodynamic properties of the driver gas, we assume that the detonation products are in chemical equilibrium above T=1,800 K at which point the composition is frozen.

Here, we approximate internal energy as only a function of temperature. This assumption, which is characteristic of the ideal gas regime, does not include a weak pressure dependence in the combustion products properties; however, most of the reactions in the present context occur at low pressure after the detonation products have expanded the mixture. For more details on the specific approximations to the thermodynamics see [8].

For most of the simulation, we can model the gaseous component of the flow using an ideal gas approximation. This approximation is not, however, valid for the detonation products at early time. For the detonation products, we use the temperature-based form of the JWL discussed by Menikoff [10]

$$p_{jwl} = Ae^{-R_0\rho_0/\rho} + Be^{-R_1\rho_0/\rho} + \omega c_v \rho T$$

which explicitly expresses the pressure in terms of density and temperature.

As noted above, it is assumed that reactions occur on a much faster time scale than the fluid mechanics; i.e., mixtures of fuel and air instantly react to products. The reaction process is controlled by mixing and combustion occurs at near stoichiometric conditions. Thus, to model the combustion process in regions where fuel and oxidizer are both present, we simply transform the available fuel and oxidizer to products in stoichiometric proportion until either fuel or oxidizer is exhausted. Although with our given normalization the internal energy is not changed by the combustion process, the temperature increases dramatically to maintain a constant (local) energy. The empirical models for the volatilzation of the aluminum allow that time scale to be treated explicitly.

Numerical methodology

The above equations for the multiphase model were integrated using a high-order Godunov scheme. The basic integration methodology is coupled to a structured adaptive mesh refinement (AMR) [1] algorithm that allows us to follow Geometry of the calorimeters is modeled using an embedded boundary approach that represents the domain boundary as an interface in a regular computational mesh. The overall computational method is discussed in Pember et al. [14]. the thin reaction zones and detonations on the computational grid. The methodology is parallelized using a coarse-grained data-distribution approach in which three-dimensional grid patches are distributed to processors [17].

It is well known that the system of equations considered here has an eigenvector deficiency and consequently is not a classical well-posed hyperbolic system (although the phase interaction terms appear to stablize the system). This introduces additional considerations when constructing a Riemann solver for use in the Godunov algorithm. We have use the approach of Collins et al. [4] for the simulations presented here. We do not include explicit viscous terms so that the simulations implicitly incorporate an Integrated Large Eddy Simulation (ILES) type representation of mixing, described by Boris et al. [3], which is a reasonable approximation to the high Reynolds and Peclet numbers associated with the post-detonation environment.

The equation of state solves for the equilibrium temperature given the overall gas phase mixture energy and composition and then computes pressure using the resulting temperature and density. The interphase exchange terms are included using a Strang-splitting approach. The combustion component of the model occurs after the fluid mechanics step using the algorithm describe above.

The computations were performed in three stages. For the early blast-wave phase of the computation, four levels of refinement were used for an effective resolution of approximately 0.2 mm. After the initial charge has expanded to approximately eight charge radii, the resolution was reduced to 0.4 mm. After the blast wave has expanded to approximate 7cm in radius, the resolution is reduced to approximately 0.8 mm for the remainder of the simulation.

3. Results

We consider two calorimeter configurations. The first (Case C) is a cylinder approximately 21 cm high with a diameter of 20 cm, which has a volume of 6.6 liters. The other configuration (Case T) is 100 cm long tunnel with an 8 cm square cross-section. For each case the driver is a 0.5 g spherical PETN charge with radius

0.49 cm described with a JWL equation of state as noted above. The aluminum is located in cylindrical shell around the charge of radius 0.7 cm and height of 1.4 cm, oriented with the axis of the cylinder aligned vertically. The cylinder contains 1 g of aluminum in a volume of 1.65 cm^3, corresponding to a volume fraction of approximately 22.4%. For both cases the charge is located in the center of the domain. These cases are from an experimental study of Neuwald et al. [11]. The two cases considered represent distinctly different geometries and enable us to assess the influence of overall domain geometry on the effectiveness of the SDF charge.

In Figure 1 and 2 we show the temperature field along centerline cuts for cases C and T, respectively. The high temperature regions highlighted in the figures coincide with the location of the combustion products and illustrate the result of the both aluminum combustion and afterburning of the PETN detonation product gases. Figure 4 shows the time history of integrated composition of the gas for both cases. For case C, the combustion process is highly efficient with most of the aluminum and detonation product gases being consumed by the end of the simulation. For the tunnel case T, the combustion efficiency has been considerably reduced. For this geometry, only 40% of the aluminum and litte of the detonation product gases are consumed. The reason for this is evident in the visualizations of the different components of the mixture shown in Figure 3. At t=2.5 msec, the remaining oxidizer is located at the ends of the tunnel, while the fuel is localized to the center. There is a zone of combustion product separating the fuel and oxidizer, effectively quenching the reactions.

In Figure 5 we compare pressure data from the simulations with measurement from two calorimeter experiments. In both cases, we compare with data from [16] For these comparisons, we have shifted the simulation data in time by 26 μsec and 106 μsec, for cases C and T, respectively. There are several possible explanations for the early arrival of the initial blast wave. The assumptions of a dispersed particle phase is not valid at early time. It is also the case that the ignition of the aluminum is not fully understood. Either of these issues could contribute to changing the timing of the initial wave. Finally, there is considerable uncertainty in the interphase coupling terms. Although the models have been reasonable well calibrated for spherical particles, characterization of the model for flake aluminum used here is less well understood. Subject to the temporal shift of the data, the simulated pressre traces agree well with the experimental data, particularly for Case C. For case T, the experimental traces are somewhat delayed and weaker than the simulated results. We conjecture that this lag is caused by heat transfer to the tunnel walls that are not being modeled in the simulation.

4. Summary

In this paper, we have considered a shock-dispersed fuel explosive in which a small driver charge is used to disperse aluminum particles that burn in the ambient atmosphere. We have modeled this process using a multiphase model in which the aluminum is treated as a dispersed solid phase that does not support pressure. We have developed a three-dimensional AMR code that simulates this sytems. Three-dimensional simulations using this algorithm were presented for two calorimeter geometries to illustrate the role of gross domain geometry on the combustion process. With the exception of a temporal shift of the initial shock arrival time, the simulations agree well with experimental data. In our previous simulations on single-phase gaseous systems, the ILES type approach we are using is essentially scale invariant. For the multiphase system considered here, the particle size introduces an additional length scale. Future work will examine how the performance of aluminum SDF charges changes as the system size is increased.

References

[1] J. Bell, M. Berger, J. Saltzman, and M. Welcome. A three-dimensional adaptive mesh refinement for hyperbolic conservation laws. *SIAM Journal on Scientific and Statistical Computing*, 15(1):127–138, 1994.

[2] J. B. Bell, M. S. Day, V. E. Beckner, C. A. Rendleman, A. L. Kuhl, and P. Neuwald. Numerical simulation of the combustion of PETN/TNT products with air in closed chambers. *ICDERS–20, Montreal, Canada*, 2005.

[3] J. Boris, F. Grinstein, E. Oran, and R. Kolbe. New insights into large eddy simulation. *Fluid Dynamics Research*, 10, 1992.

[4] P. Collins, R. E. Ferguson, K. Chien, A. L. Kuhl, J. Krispin, and H. M. Glaz. Simulation of shock-induced dusty gas flows using various models. *AIAA Fluid Dynmics Conference, AIAA 94-2309*, 1994.

[5] L. E. Fried, P.C. Souers, W.M Howard, and P. Vitello. LLNL CHEETAH Code. `http://www-cms.llnl.gov/s-t/cheetah.html`.

[6] A. L. Kuhl, J. B. Bell, V. E. Beckner, and B. Khasainov. Simulation of turbulent fields of shock-dispersed aluminum using the amr code. *41st JANNAF (2A) CS-III*, 3, 2006.

[7] A. L. Kuhl, M. Howard, and L. Fried. Thermodynamic model of afterburning in explosions. *Energetic Materials, 34th ICT Conference*, pages 74.1–74.14, 2003.

[8] A. L. Kuhl and B. Khasainov. Quadratic model of thermodynamic states in SDF explosions. *Energetic Materials, 38th ICT Conference*, 2007.

[9] A. L. Kuhl, B. Khasainov, and J. B. Bell. Two-phase model for combustion in explosions. *Energetic Materials, 37th ICT Conference*, 2006.

[10] R. Menikoff. Comparison of consitutive models fpr pbx 9501. Technical Report LA-UR-06-2355, Los Alamos National Laboratory, Los Alamos, NM, 2006.

[11] P. Neuwald, H. Reichenbach, and A. L. Kuhl. Shock-dispersed fuel charges combustion in chambers and tunnels. *Energetic Materials, 34th ICT Conference*, pages 13.1–13.14, 2003.

[12] R. I. Nigmatulin. *Dynamics of Multi-phase Flows, Vol. 1.* Moscow: Nauka, 1987.

[13] D. L. Ornellas. Calorimetric determination of the heat and products of detonation for explosives: October 1961 to April 1982. Technical Report UCRL-52821, Lawrence Livermore National Laboratory, Livermore, CA, 1984.

[14] R.B. Pember, J.B. Bell, P. Colella, W.Y. Crutchfield, and M.L. Welcome. An adaptive cartesian grid method for unsteady compressible flow in irregular regions. *J. Comp. Phys.*, 120(2):278–304, September 1995.

[15] F. H. Ree, W. J. Pitz, M. van Thiel, and P. C. Souers. Over-abundance of carbon monoxide in calorimeter tests. *J. Phys. Chem.*, 100:5761–5765, 1996.

[16] H. Reichenbach, P. Neuwald, and A. L. Kuhl. Waveforms measure in confined thermobaric explosions. *Energetic Materials, 38th ICT Conference*, 2007.

[17] Charles A. Rendleman, Vincent E. Beckner, Mike Lijewski, William Y. Crutchfield, and John B. Bell. Parallelization of structured, hierarchical adaptive mesh refinement algorithms. *Computing and Visualization in Science*, 3(3):147–157, 2000.

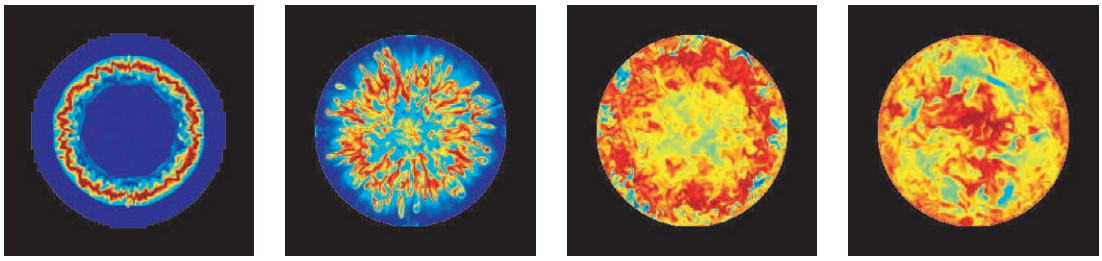


Figure 1: Temperatures for case C at t = 3.00e-05, 1.00e-4, 4.00e-04 and 2.50e-03. Temperature range is from 273K (dark blue) to 4200K (red).

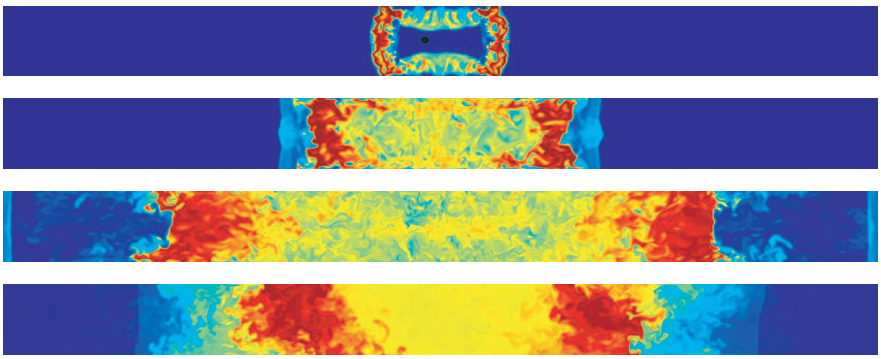


Figure 2: Temperatures for case T at t = 3.e-05, 1.00e-4, 4.00e-04 and 2.50e-03. Temperature range is from 273K (dark blue) to 4200K (red).

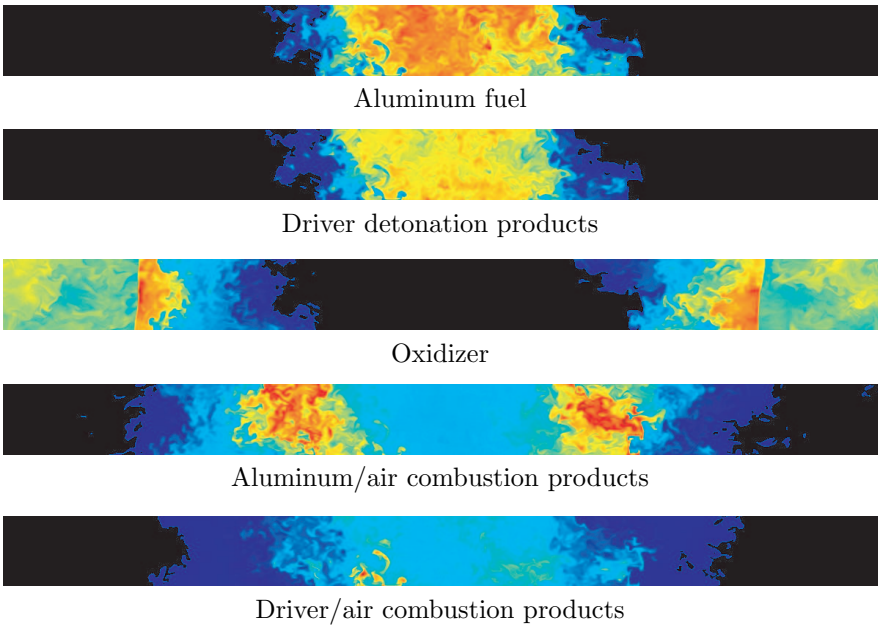


Figure 3: Gas composition for case T at t=2.5 msec

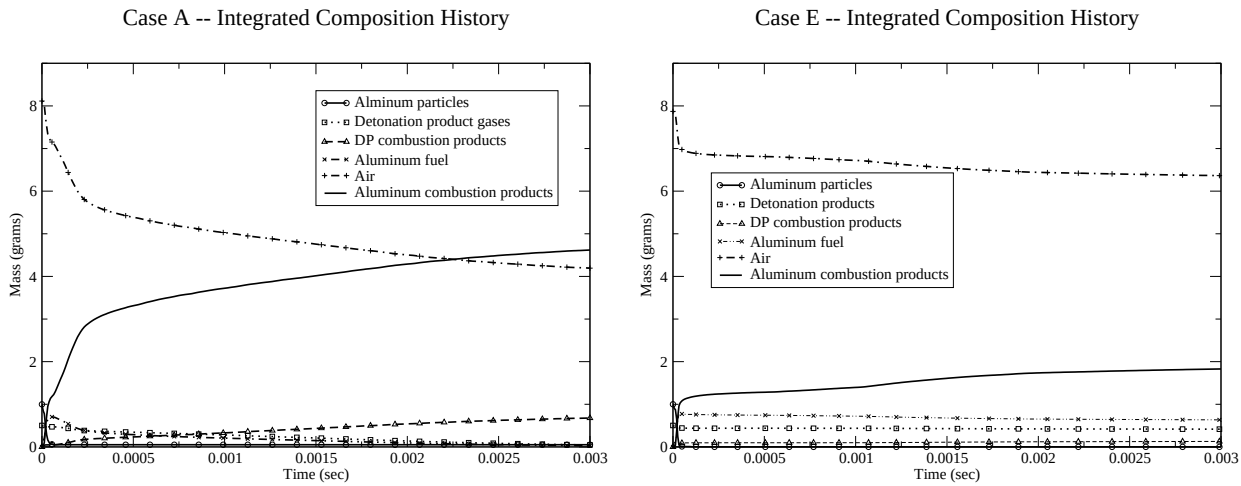


Figure 4: Integrated gas components and aluminum particle density for Case C (a) and Case T (b).

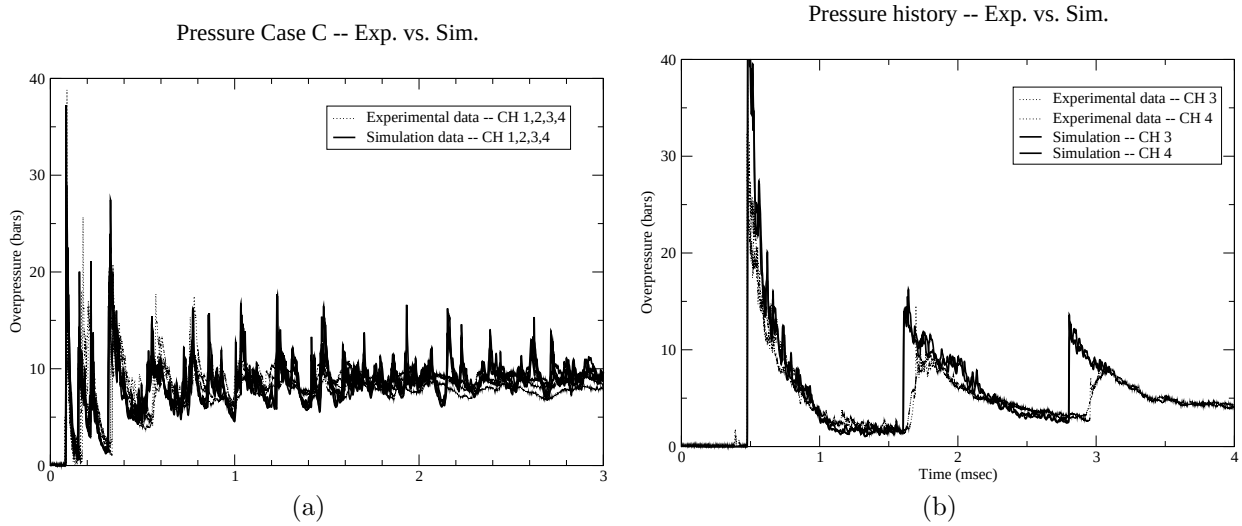


Figure 5: Comparison of pressure traces with experimental data for Case C (a) and Case T (b). Experimental data courtesy of P. Neuwald. Simulation data for case C is shifted 26 *mu*sec and case T is shifted 106 *mu*sec.